World Academy of Science, Engineering and Technology
International Journal of Chemical and Molecular Engineering
Vol:12, No:11, 2018

One Dimensional Reactor Modeling for Methanol Steam Reforming to Hydrogen

Hongfang Ma, Mingchuan Zhou, Haitao Zhang, Weiyong Ying

***Abstract*—**One dimensional pseudo-homogenous modeling has been performed for methanol steam reforming reactor. The results show that the models can well predict the industrial data. The reactor had minimum temperature along axial because of endothermic reaction. Hydrogen productions and temperature profiles along axial were investigated regarding operation conditions such as inlet mass flow rate and mass fraction of methanol, inlet temperature of external thermal oil. Low inlet mass flow rate of methanol, low inlet temperature, and high mass fraction of methanol decreased minimum temperature along axial. Low inlet mass flow rate of methanol, high mass fraction of methanol, and high inlet temperature of thermal oil made cold point forward. Low mass fraction, high mass flow rate, and high inlet temperature of thermal oil increased hydrogen production. One dimensional models can be a guide for industrial operation.

***Keywords*—**Reactor, modeling, methanol, steam reforming.

I. Introduction

METHANOL can be reformed with water steam to produce hydrogen. Hydrogen is considered as an alternative fuel due to high energy content per mass unit and low emissions, which has a strategic importance for pursuing environment benign, clean and sustainable energy system [1]. However, the storage and transportation of hydrogen still belong to a non-solved issue. For all known hydrogen storage materials, methanol can be a promising energy carrier, which has high H/C ratio [2]-[4]. Additional, methanol reforming to hydrogen is performed at low temperature unlike methane reforming [5]. Hence, methanol steam reforming (MSR) is a preferable technology for hydrogen generation from hydrogen carrier.

Considering the application of hydrogen production, by-product CO should be minimized, which satisfies the MSR's favorable thermodynamics at low temperature [6]. Cu-based catalysts are the most commonly used for MSR reaction due to high activity and selectivity [7]. For improving catalytic performance, many researches are reported in the literature based on the addition of promoters and preparation method [8], [9]. With efforts, $CuO/ZnO/Al_2O_3$ catalysts have been commercialized with co-precipitation method, which has desirable performance for MSR.

Different types of reactors have been applied for MSR reaction to obtain different purposes. Micro-channel reactor with well-coated catalysts can provide hydrogen for micro-scale fuel cell [10]. Better heat transfer and mass transfer in micro scale reactor disappears as system output increases owing to scale factor. Membrane reactor has been focused on for MSR reaction [11], especially palladium-based membrane reactor [12], which may have high cost. Fixed-bed reactor is the simplest reactor type for industrial manufacture. Researchers master enough experience to design reactor on large scale. Hence, fixed-bed reactor still belongs to main trends for producing hydrogen massively.

In this paper, one-dimensional model for fixed-bed reactor with MSR reaction was established to display reactor behavior. Parametric study was carried out to figure out temperature and concentration variation along axial with respect to inlet mass flow rate and mass fraction of methanol, inlet temperature of external thermal oil.

II. Mathematical Model

A. Reactor Description

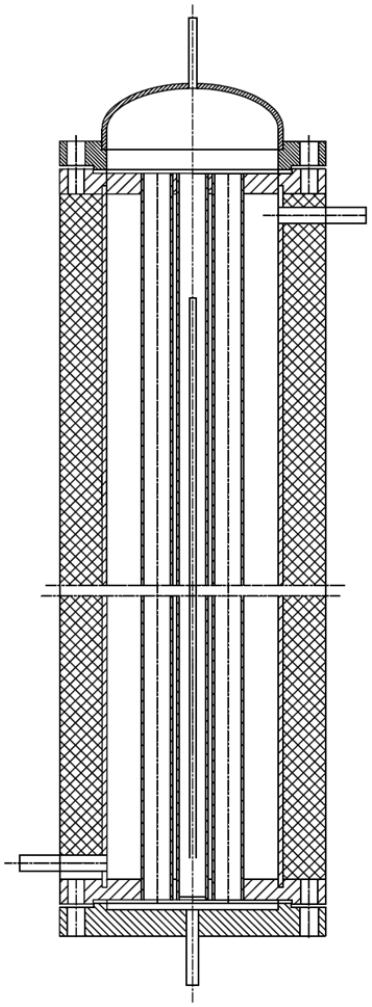

Fig. 1 The structure of MSR reactor

Hongfang Ma is with the East China University of Science and Technology, China (e-mail: mark@ecust.edu.cn).

Fig. 1 displays the structure of fixed-bed reactor for MSR. The reactor belongs to tubular fixed-bed reactor. Considering endothermic reaction of MSR, thermal oil was provided in shell side to maintain reaction temperature. The catalyst was loaded in tube. The mixture of methanol and water passed through catalyst bed from upside to downside to produce hydrogen and by-product. The heat was exchanged between catalyst bed and thermal oil in counter flow. According to plant operation, the reactor structure data and operation conditions have been listed in Table I.

TABLE I
REACTOR STRUCTURE DATA AND OPERATION CONDITIONS

Parameters		Value
Tube dimension (m)		0.038×0.0025
Number of tubes		584
Reactor inner diameter (m)		1.3
Reactor length (m)		5.6
Pressure (MPa)		1.9
Mass flow rate of methanol (kg/h)		394
Volume flow rate of thermal oil (m^3/h)		75
	Case 1	Case 2
Feed inlet temperature (K)	517	513
Thermal oil inlet temperature (K)	527	523
Mass fraction of CH_3OH	0.445	0.435

B. Reactor Model

In this study, a one-dimensional pseudo-homogeneous model has been considered for steady state simulation of MSR reactor. The basic structure of this model contains heat and mass equations coupled with kinetic equations. The predictions of physical properties are obtained from the Perry's chemical engineers' handbook [13].

The mathematical model is developed based on the following assumptions:

(1) It is irrespective of the concentration and temperature variations in radial direction.
(2) Heat losses to the surrounding are neglected.
(3) There are no interfacial gradients of temperature and concentration between solid and gas phases
(4) The temperature radial profiles of thermal oil on shell side are uniform.

The mass and heat balances in fixed-bed reactor are expressed by the following equations.

Mass balance:

$$\mathrm{d}N_{CO} = Am_t\rho_b dlR_{CO} \tag{1}$$

$$\mathrm{d}N_{CO_2} = Am_t\rho_b dlR_{CO_2} \tag{2}$$

Energy balance:

Tubular side:

$$N_T C_{pb} dT_b = dN_{CO}\left(-\Delta H_{RCO}\right) + dN_{CO_2}\left(-\Delta H_{RCO_2}\right) + K_{bo} m_t \pi D_t (T_o - T_b) dl \tag{3}$$

Shell side:

$$N_o C_{po} dT_o = K_{bo} m_t \pi D_t (T_b - T_o) dl \tag{4}$$

At the inlet, the velocity, temperature, components of the reactor inlet can be calculated based on the boundary conditions of the reactor inlet. The following initial conditions are applied at inlet:

At l=0

$$y_i = y_{i,0} \tag{5}$$

$$T_b = T_{b,0} \tag{6}$$

$$T_o = T_{o,0} \tag{7}$$

The global kinetics of MSR have been developed by Wu [14], [15]. The generation rates of CO and CO_2 are given by (8) and (9). Referenced parameters of global kinetics of MSR are listed in [15].

$$R_{CO} = \frac{dN_{CO}}{dW} = k_1 f_m^{a_1}(1-\beta_1) \tag{8}$$

$$R_{CO_2} = \frac{dN_{CO_2}}{dW} = k_2 f_m^{a_2} f_{H_2O}^{a_3}(1-\beta_2) \tag{9}$$

$$k_1 = k_{0,1}\exp(\frac{E_1}{R_g T}) \tag{10}$$

$$k_2 = k_{0,2}\exp(\frac{E_2}{R_g T}) \tag{11}$$

$$\beta_1 = \frac{f_{CO} f_{H_2}^2}{f_m K_{f1}} \tag{12}$$

$$\beta_2 = \frac{f_{CO_2} f_{H_2}^3}{f_m f_{H_2O} K_{f2}} \tag{13}$$

$$K_{f1} = \exp(-22.696 - \frac{8982.426}{T} + 7.698 ln T - 3.922\times10^{-3} T - 5.132\times10^{-7} T^2 + 5.132\times10^{-10} T^3)/0.101325^2 \tag{14}$$

$$K_{f2} = \exp(-17.655 - \frac{4211.466}{T} + 5.753\ln T + 1.709\times10^{-3} T - 2.684\times10^{-7} T^2 + 7.237\times10^{-10} T^3)/0.101325^2 \tag{15}$$

C. Simulation Method

The one-dimensional models were calculated by MATLAB software to demonstrate hydrogen production and temperature profiles along axial. The ordinary differential equations can be solved by 4th order Runge-Kutta method.

III. Results and Discussion

A. Model Validation

The experimental data from plant were used to validate one dimensional model, which was calculated to simulate the

reactor at the operating conditions as the same as plant operation. Table II shows that the comparisons of the simulated results and the experimental data. The calculated compositions of outlet gas are in accord with the experimental values. The exit temperature also has good agreement between the one-dimensional model and plant. Fig. 2 displays temperature and hydrogen production profiles along axial in case 1. The temperature of catalyst bed decreased along axial in foreside of reactor because of endothermic reaction and low heat transfer rate from catalyst bed to thermal oil. The coldest temperature of 501.7 K was located at 1.1 m of bed length and had 16 K lower than the inlet temperature. Beyond the cold point, high temperature difference between catalyst bed and thermal oil made the temperature of catalyst bed increased. The hydrogen production increased along axial and hydrogen production can achieve 727 Nm^3/h at exit.

TABLE II
COMPARISON OF THE RESULTS AT REACTOR OUTLET FROM CALCULATED (CAL.) WITH INDUSTRIAL PRACTICAL (IND.) DATA

Parameters	Case 1			Case 2		
	Ind. data	Cal. data	Relative error (%)	Ind. data	Cal. data	Relative error (%)
CH_3OH[a] (wt %)	14	13.49	-3.64	15	16.03	6.86
CO[b] (mol %)	0.20	0.21	5.00	0.20	0.20	0.00
CO_2[b] (mol %)	24.85	24.84	0.04	24.85	24.85	0.00
H_2[b] (mol %)	74.95	74.95	0.00	74.95	74.95	0.00
Temperature at exit (K)	513	513.1	0.02	509	509.4	0.07

[a] mass fraction of liquid production at exit.
[b] mole fraction of dry-based product gas.

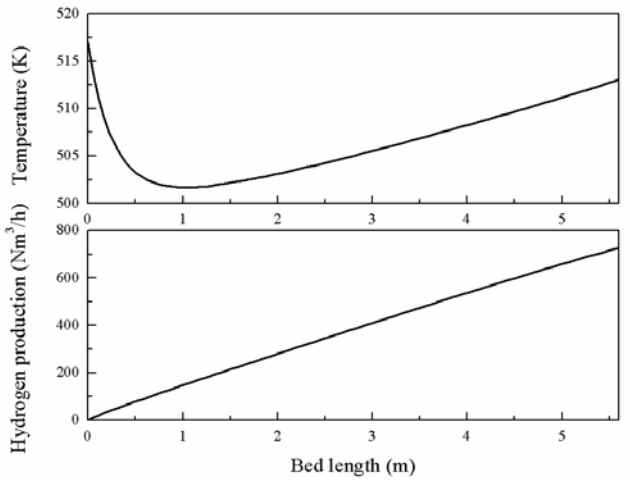

Fig. 2 Temperature and hydrogen production profiles along axial in case 1

B. Effect of Inlet Mass Flow Rate of Methanol

Fig. 3 shows temperature profiles along axial versus different mass flow rate of methanol. Low mass flow rate decreased the temperature of cold point. The position of cold point moved backward. In Fig. 4, high mass flow rate increased hydrogen production. At 294 kg/h mass flow rate of methanol, the conversion of methanol achieved 100% near reactor exit leading to dramatically increase the temperature of catalyst bed.

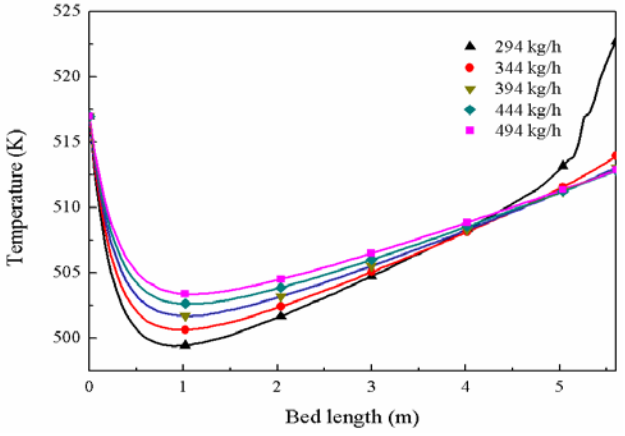

Fig. 3 Temperature profiles along axial versus different mass flow rate of methanol

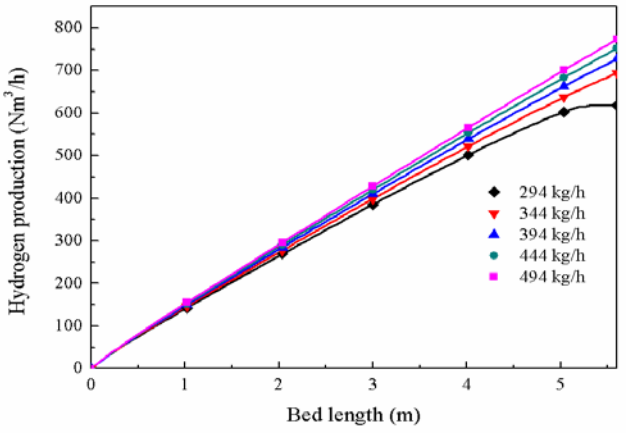

Fig. 4 Hydrogen production profiles along axial versus different mass flow rate of methanol

C. Effect of Mass Fraction of Methanol

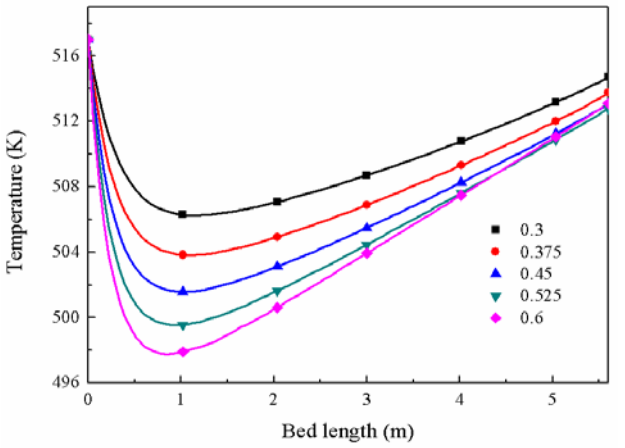

Fig. 5 Temperature profiles along axial versus different mass fraction of methanol

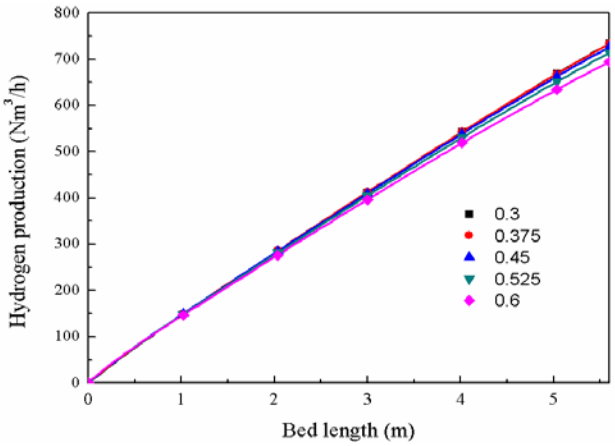

Fig. 6 Hydrogen production profiles along axial versus different mass fraction of methanol

Fig. 5 displays temperature profiles of catalyst bed as the function of mass fraction of methanol. Low mass fraction of methanol increased the temperature of catalyst bed due to large gas bulk. Low temperature of cold point at high mass fraction made cold point forward because of high temperature difference. Different mass fraction of methanol had a little influence on hydrogen production, as shown in Fig. 6. Low mass fraction of methanol can increase hydrogen production slightly.

D.Effect of Inlet Temperature of External Thermal Oil

Temperature profiles along axial are displayed in Fig. 7. Different inlet temperature of thermal oil had obvious change on temperature of catalyst bed. High inlet temperature increased temperature profiles along axial and made cold point forward due to high temperature difference between catalyst bed and thermal oil. High temperature can accelerate reforming reaction. High inlet temperature of thermal oil can increase hydrogen production, as shown in Fig. 8. At 497 K inlet temperature of thermal oil, conversion of methanol had achieved 100% before reaction exit, which led to dramatic increase of bed temperature at reaction exit due to no endothermic reaction. Exorbitant inlet temperature of thermal oil had no benefit for hydrogen production.

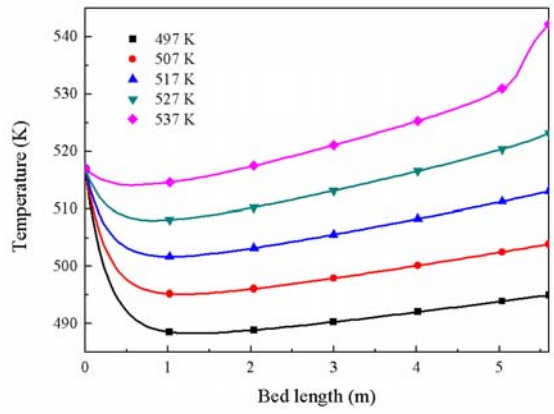

Fig. 7 Temperature profiles along axial versus different inlet temperatures of thermal oil

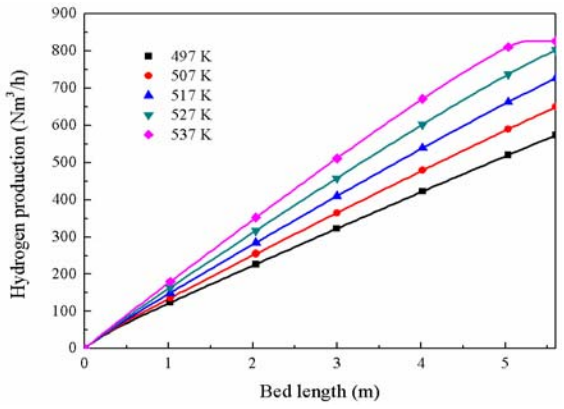

Fig. 8 Hydrogen production profiles along axial versus different inlet temperatures of thermal oil

IV. Conclusions

One dimensional pseudo-homogenous model was established for fixed-bed reactor of MSR, and the simulation was carried out to investigate reactor behavior as function of inlet mass flow rate of methanol, mass fraction of methanol and inlet temperature of thermal oil. The simulation results indicated that the mathematic model can match well with industrial data. High inlet mass flow rate of methanol, low mass fraction of methanol led to high temperature at catalyst bed and made cold point backward. At high inlet temperature of thermal oil, the temperature of catalyst bed became high and cold point moved forward. Low mass fraction, high mass flow rate of methanol, and high inlet temperature of thermal oil had benefit for more hydrogen production.

Nomenclature

A	Catalyst bed cross section area, m^2
C_p	Heat capacity at constant pressure, kJ/(kmol·K)
D_t	Inner diameter of tube, m
E	Activation energy, kJ/mol, 1 kJ/mol=1000 J/mol
f	Fugacity, MPa, 1 MPa=10^6 Pa
K_{bo}	Heat transfer coefficient between catalyst bed and thermal oil, $W/(m^2 \cdot K)$
K_f	Reaction equilibrium constant
k_0	Pre-exponential factor
l	Reactor length, m, independent variable
m	Number of tube
N	Mole flow rate, koml/h, 1 mol/s=3.6 kmol/h
P	Pressure, MPa
R_g	Gas constant, J/(mol·K)
R	Reaction rate, kmol/(kg•h), 1 mol/(kg_c•s)=3.6 kmol/(kg_c•h)
T	Temperature, K
W	Catalyst weight, kg
ΔH	Reaction enthalpy, kJ/mol
y	Mole fraction
ρ	Density, kg/m^3
Subscript	
b	Catalyst bed
i	Component
m	Methanol
o	Thermal oil

REFERENCES

[1] L. Barreto, A. Makihira, K. Riahi, "The hydrogen economy in the 21st century: a sustainable development scenario." *Int. J. Hydrogen Energy* Vol. 28, no. 3, pp. 267-284, 2003.

[2] D. R. Palo, R. A. Dagle, J. D. Holladay, "Methanol steam reforming for hydrogen production." *Chem. Rev.* Vol. 107, no. 10, pp. 3992-4021, 2007.

[3] R. D. Cortright, R. Davda, J. A. Dumesic, "Hydrogen from catalytic reforming of biomass-derived hydrocarbons in liquid water." *Nature* Vol. 418, no. 6901, pp. 964-967, 2002.

[4] M. C. Denney, V. Pons, T. J. Hebden, D. M. Heinekey, K. I. Goldberg, "Efficient catalysis of ammonia borane dehydrogenation." *JACS* Vol. 128, no. 37, pp. 12048-12049, 2006.

[5] L. Barelli, G. Bidini, F. Gallorini, S. Servili, "Hydrogen production through sorption-enhanced steam methane reforming and membrane technology: a review." *Energy* Vol. 33, no. 4, pp. 554-570, 2008.

[6] B. A. Peppley, J. C. Amphlett, L. M. Kearns, R. F. Mann, "Methanol–steam reforming on $Cu/ZnO/Al_2O_3$. Part 1: the reaction network." *Appl. Catal., A* Vol. 179, no. 1, pp. 21-29, 1999.

[7] S. Sá, H. Silva, L. Brandão, J. M. Sousa, A. Mendes, "Catalysts for methanol steam reforming—a review." *Appl. Catal., B* Vol. 99, no. 1, pp. 43-57, 2010.

[8] G.-S. Wu, D.-S. Mao, G.-Z. Lu, Y. Cao, K.-N. Fan, "The role of the promoters in Cu based catalysts for methanol steam reforming." *Catal. Lett.* Vol. 130, no. 1-2, pp. 177-184, 2009.

[9] C.-Z. Yao, L.-C. Wang, Y.-M. Liu, G.-S. Wu, Y. Cao, W.-L. Dai, H.-Y. He, K.-N. Fan, "Effect of preparation method on the hydrogen production from methanol steam reforming over binary Cu/ZrO_2 catalysts." *Appl. Catal., A* Vol. 297, no. 2, pp. 151-158, 2006.

[10] A. Kundu, J. Park, J. Ahn, S. Park, Y. Shul, H. Han, "Micro-channel reactor for steam reforming of methanol." *Fuel* Vol. 86, no. 9, pp. 1331-1336, 2007.

[11] A. Iulianelli, P. Ribeirinha, A. Mendes, A. Basile, "Methanol steam reforming for hydrogen generation via conventional and membrane reactors: a review." *Renewable Sustainable Energy Rev.* Vol. 29, no., pp. 355-368, 2014.

[12] Y.-M. Lin, M.-H. Rei, "Study on the hydrogen production from methanol steam reforming in supported palladium membrane reactor." *Catal. Today* Vol. 67, no. 1, pp. 77-84, 2001.

[13] D. W. Green, "Perry's Chemical Engineers' Handbook," New York: McGraw-hill, 2008.

[14] Q. Wu, S. Wang, B. Zhu, Z. Zhu, Y. Zhong, "Thermodynamics Analysis of Hydrogen Production by Catalytic Decomposition and Steam Reforming of Methanol." *Journal of East China University of Science and Technology (Natural Science Edition)* Vol. 29, no. 2, pp. 120-123, 2003.

[15] Q. Wu, S. Wang, B. Zhu, Z. Zhu, Y. Zhong, "Study on the Global Reaction Kinetics of Hydrogen Production by Methanol Steam Reforming." *Petrochemical Technology* Vol. 32, no. 6, pp. 483-486, 2003.